RSC Advances

PAPER

View Article Online
View Journal | View Issue

Cite this: *RSC Adv.*, 2016, **6**, 28593

Bridged bis(β-cyclodextrin)s-based polysaccharide nanoparticles for controlled paclitaxel delivery†

Li-Xia Chen,[a] Ying-Ming Zhang,[a] Yu Cao,[a] Heng-Yi Zhang[a] and Yu Liu*[ab]

Received 29th January 2016
Accepted 10th March 2016

DOI: 10.1039/c6ra02644c

www.rsc.org/advances

The lack of effective and specific carriers is generally considered as the main obstacle hindering further clinical applications in cancer therapy. In this work, a novel polysaccharide nanocarrier was successfully constructed by the noncovalent complexation of disulfide-containing bridged bis(β-cyclodextrin)s with adamantane-grafted hyaluronic acid. Possessing a three-dimensional hydrophobic microenvironment, the obtained binary nanoparticles could serve as a biocompatible platform for the loading and solubilizing of paclitaxel. More interestingly, spectroscopic and microscopic experiments revealed that the hydrophobic drug could be completely released from the nanocarrier through disulfide bond cleavage and enzymatic degradation. In addition, the active hyaluronic acid units endowed the resultant nanoparticles with desirable cell-specific targeting ability, thus leading to a relatively better anticancer activity toward tumor cells than free paclitaxel. We envision that the present work will provide a new method in the fabrication of more advanced macrocycle-based drug carriers.

Introduction

Despite the fact that significant progress has been made in the design of functional drug carriers, some crucial optimization and implementation challenges still remain for the development of controlled and targeted drug delivery systems.[1–3] Nowadays, researchers have become aware of the importance of biocompatible and multistimuli-responsive nanomaterials to achieve synergistic therapeutic effects in physiological environments.[4–8] In this context, the construction of carrier-mediated artificial systems decorated with active targeting sites provides a powerful strategy to overcome current drawbacks in drug formulation and delivery. Among the numerous building blocks in the construction of bioactive hybrid materials, the macrocycle-based drug carriers are particularly attractive and may confer distinct practical superiorities, because the commonly employed macrocycles, such as cyclodextrin (CD) and cucurbituril, possess an inherently hydrophobic cavity to form simple inclusion complexes and highly ordered supramolecular assembled entities, thus leading to the enhancement in drug solubility, stability, and bioavailability.[9] In particular, the bridged bis(β-CD)s bearing two cavities in close vicinity with a functional linker, as compared to the native and mono-modified analogues, can significantly promote the original binding affinity and molecular selectivity toward various organic and biological substrates, including dyes, oligopeptides, steroids, and drug molecules.[10] Thus, it is believed that the rational integration of bridged bis(β-CD)s with cell-specific targeting ligands will be developed into a new approach to transport administrated drug molecules.

In our recent studies, we have demonstrated a versatile nanoplatform for the targeted delivery of anticancer drugs originating from the polysaccharide–gold nanocluster supramolecular conjugates, which showed pH-responsive drug release behaviors and targeted tumor cell inhibition abilities due to the hyaluronic acid (HA) reporter-mediated endocytosis.[11] These findings inspired us to hypothesize that the construction of a polysaccharide-based multistimuli-responsive nanocarrier may be achieved by introducing some appropriate bridged bis(β-CD)s as cross-linkers. In this work, the adamantane-grafted HA (HAADA) was intermolecularly connected with the disulfide-containing bridged bis(β-CD)s (DTCD) to construct a binary dual-stimulus responsive polysaccharide nanoparticle, which can be utilized as a functional nanocarrier to encapsulate the water insoluble paclitaxel (PTX) with a moderate loading capacity. Therefore, benefiting from the redox-active disulfide bonds and biocompatible HA skeleton, the drug molecules could be completely released through the disulfide bond cleavage and enzymatic degradation.[12–14] Superior to free PTX, the introduction of nanocarrier can not only greatly enhance the water solubility of drug molecules, but also empower them the targeting ability to specifically recognize the hyaluronic acid receptor expressing cancer cells.[15–17] As a result, the bridged bis(β-CD)s-based polysaccharide nanoparticle gave improved anticancer activity toward tumor cells and may find novel possibilities for the development of advanced drug

[a]*Department of Chemistry, State Key Laboratory of Elemento-Organic Chemistry, Nankai University, Tianjin 300071, P. R. China. E-mail: yuliu@nankai.edu.cn*

[b]*Collaborative Innovation Center of Chemical Science and Engineering (Tianjin), Tianjin 300071, P. R. China*

† Electronic supplementary information (ESI) available: Fig. S1–S10 and Table S1. See DOI: 10.1039/c6ra02644c

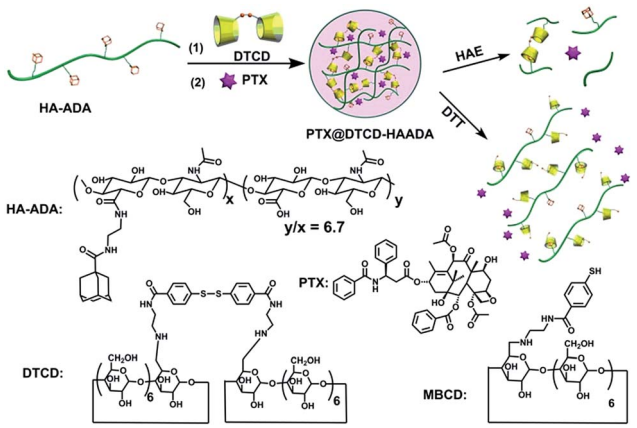

Scheme 1 Construction of PTX@DTCD·HAADA supramolecular assembly and dual-stimulus responsive drug release process.

delivery systems. The chemical structures and synthetic route for the preparation of DTCD·HAADA binary supramolecular conjugate are shown in Scheme 1.

Experimental

Synthesis of 4-mercaptobenzoic acid-modified β-CD (MBCD)

4-Mercaptobenzoic acid (154.2 mg, 1.0 mmol) and hydroxybenzotriazole (HOBt, 162.0 mg, 1.2 mmol) were dissolved in dry *N*,*N*-dimethylformamide (DMF, 40 mL) and stirred in an ice bath for 0.5 h. A solution of mono-6-deoxy-6-ethylenediamino-β-CD (1.29 g, 1.1 mmol) and *N*,*N*′-dicyclohexylcarbodiimide (DCC, 247.6 mg, 1.2 mmol) in dry DMF (10 mL) was then added dropwise. The reaction mixture was stirred at 0 °C under an N_2 atmosphere overnight, and then stirred at room temperature for another 72 h. The mixture was filtered and the filtrate was dried under reduced pressure to remove the solvent. The residue was dissolved in little water, then poured into acetone (500 mL) and the yellow precipitate was filtered. The crude product was purified by column chromatography (silica gel) by using *n*-PrOH/H_2O/25% $NH_3 \cdot H_2O$ (6 : 3 : 1 v/v/v) as the eluent. The product obtained was further purified by MPLC reversed phase with a water/ethanol (80 : 20 v/v) eluent, then targeted compound was obtained as a faint yellow solid (Scheme S1 in ESI†). ^{1}H NMR (400 MHz, DMSO-d_6, TMS): δ = 2.60–2.99 (m, 4H, –NH–CH_2CH_2–NH–), 3.44–3.84 (m, 28H, H of C-3, C-5, C-6 of β-CD), 4.49 (s, 6H, H of C6-OH of β-CD), 4.83 (s, 7H, H of C-1 of β-CD), 5.61–5.92 (m, 14H, H of C2-OH, C3-OH of β-CD), 7.60 (d, J = 8.2 Hz, 2H, H of benzene), 7.83 (d, J = 8.3 Hz, 1H, H of benzene), 7.92 (d, J = 8.3 Hz, 1H, H of benzene), 8.44 ppm (s, 2H, H of –CONH–); ^{13}C NMR (100 MHz, DMSO-d_6, TMS): δ = 48.3, 59.9, 70.0, 72.0, 72.4, 73.0, 81.5, 83.0, 101.9, 126.3, 128.3, 130.2, 133.4, 138.8, 165.8 ppm; elemental analysis calcd (%) for $C_{51}H_{80}N_2O_{35}S \cdot 7H_2O$: C 42.56, H 6.58, N 1.95; found: C 42.61, H 6.90, N 1.95; HRMS: m/z: 1312.9243 $[M + H]^+$.

Preparation and characterization of DTCD·HAADA nanoparticles

In order to prepare the binary nanoparticles, the adamantane-grafted hyaluronic acid (HAADA, 1.5 mg, containing 0.50 μmol adamantyl units) and disulfide-containing bridged bis(β-cyclodextrin)s (DTCD, 0.66 mg, 0.25 μmol) were dissolved in 1 mL Mlli-Q water. The solution was sonicated for 10 min and then filtered through a membrane filter (pore size: 0.45 μm, Millipore). The particle size of the DTCD·HAADA was measured using microscopic experiments.

Preparation of PTX-loaded nanoparticles

PTX-loaded DTCD·HAADA nanoparticles were prepared by dissolving HAADA (30 mg) and DTCD (13.2 mg) in 20 mL of Mlli-Q water, and then PTX (4 mg) was dissolved in 0.2 mL of acetonitrile and dropwise added into the nanoparticles solution. After that, the mixed solution was vigorously stirred for 24 h at room temperature in darkness. The resulting solution was filtered to remove the insoluble PTX, and the filtrate was lyophilized to determine the loading and encapsulate efficiencies. To evaluate the loading efficiency of PTX within DTCD·HAADA nanoparticles, the resultant product was dissolved in acetonitrile to extract the encapsulated PTX, because the phenyl group in DTCD overlapped with PTX at 227 nm. The PTX concentration was determined by its absorption at 227 nm by UV/Vis spectroscopy. Moreover, the drug encapsulation and loading efficiencies can be calculated using the following equations.

$$\text{Encapsulation efficiency} = 100\% \times m_{\text{drug in nanoparticles}}/m_{\text{total drug}} = 100\% \times 1.28\ \text{mg}/4.0\ \text{mg} = 32.0\%$$

$$\text{Drug loading content} = 100\% \times m_{\text{drug in nanoparticles}}/m_{\text{nanoparticles}} = 100\% \times 1.28\ \text{mg}/43.2\ \text{mg} = 3.0\%$$

In vitro release of PTX from DTCD·HAADA nanoparticles by dithiothreitol (DTT) and hyaluronidase (HAE)

To investigate if the nanoparticles could be disassembled, dithiothreitol (DTT, 10 mM, 7.7 mg) was added to DTCD solution (0.66 mg mL^{-1}, 5 mL), and the solution was stirred for 1 h at 37 °C. The resultant solution was then characterized by ESI-MS. Similarly, the DTCD·HAADA nanoparticle solution (2.16 mg mL^{-1}, 5 mL) was treated by DTT (10 mM, 7.7 mg), and then the resultant solution was characterized by DLS and AFM experiments. As for the DTT-triggered drug release, the drug-loaded nanoparticles were treated by DTT and then filtered. The filtrate was lyophilized to determine the amount of remaining PTX by UV/Vis spectroscopy.

In the case of enzyme-triggered drug release, HAADA (1.5 mg, containing 0.50 μmol adamantyl units) and DTCD (0.66 mg, 0.25 μmol) were dissolved in 10 mL Mlli-Q water. The solution was sonicated for 10 min. After that, hyaluronidase (HAE) was added (the final concentration of HAE was 0.5 IU mL^{-1}), and the solution was stirred for 3 h at 37 °C. The obtained solution was then subjected to microscopic characterization.

In the release profiles, each sample solution (5 mL, [PTX] = 0.024 mg mL^{-1}) dissolved in PBS (pH = 7.2, I = 0.01 M, containing 0.3% DMSO) was placed in a dialysis membrane (M_W cut

off = 8000–14 000) and tightly sealed, which was immersed into 200 mL PBS in a beaker. At selected time intervals, 3 mL sample was taken out from buffer solution outside the dialysis bag and supplemented with 3 mL fresh buffer solution. The amount of released PTX was monitored by UV/Vis spectra absorbance at 227 nm.

Cytotoxicity experiments

HepG2 human breast cancer cells, NIH3T3 mouse embryonic fibroblasts were cultured in Dulbecco's modified Eagle's medium (DMEM), which was supplemented with 10% fetal bovine serum (FBS), in 96-well plates (2×10^4 cells per mL, 0.1 mL per well) at 37 °C under a humidified atmosphere with CO_2 (5%) for 24 h. Next, the cells were incubated with PTX, DTCD·HAADA, and PTX-loaded DTCD·HAADA ([PTX] = 2.5 μg mL^{-1}, [DTCD·HAADA] = 80 μg mL^{-1}). After incubation for 24 h, the relative cellular viability was measured using a cell-counting assay. The cell inhibitory rates were determined by the MTT assay in the evaluation of anticancer activities. The value of half maximal inhibitory concentration (IC_{50}) was calculated by GraphPad Prism software.

Results and discussion

Formation of binary supramolecular assembly

4,4′-Dithiodibenzoic acid-bridged bis(β-CD)s (DTCD) and hyaluronated adamantane (HAADA) were prepared by amidation reaction according to the previously reported methods.[18] HAADA carried adamantyl moieties at every 7.7 repeating units, and the appropriate degree of substitution can ensure both water solubility and cell targeting ability at the same time.[16] In addition, the newly synthesized 4-mercaptobenzoic acid-modified β-CD (MBCD) was used as reference compound, which was comprehensively characterized by NMR, mass spectroscopy, and elemental analysis (Fig. S1–S3 in ESI†). Next, ^1H NMR experiments were performed to demonstrate the formation of supramolecular nanoparticles by host–guest complexation of DTCD with HAADA. When mixed at 1 : 1 molar ratio, it is found that the adamantyl protons of HAADA showed significant downfield shifts and the NMR signals were drastically broadened upon addition of DTCD, suggesting the strong hydrophobic interactions between DTCD and HAADA (Fig. S4 in ESI†). Furthermore, the morphological information was visually obtained using atomic force microscopy (AFM) and transmission electron microscopy (TEM). As shown in Fig. 1a, b, d and e, free HAADA gave a scattered amorphous morphology but comparatively, many uniform dispersed spherical nanoparticles were clearly observed with diameter around 200 nm in the presence of DTCD. These results demonstrate that HAADA could be intermolecularly cross-linked into relatively large-sized nanoparticles by bridged bis(β-CD)s. Along with the microscopic investigations in the solid state, the dynamic light scattering (DLS) measurements show that the average hydrodynamic diameters of HAADA polymer decreased from 289 to 231 nm in the presence of TDCD, further indicative of the more compact structure of DTCD·HAADA assembly (Fig. 1c and f). Meanwhile, the Tyndall effect was also observed with great enhancement upon complexation of DTCD with HAADA, further indicative of the formation of large-sized aggregates in solution (Fig. S5 in ESI†). Therefore, assuming the 1 : 1 complex stoichiometry between β-CD unit and pendant adamantane, the supramolecular nanoparticle could be conveniently fabricated *in situ* by simply mixing DTCD and HAADA in water.

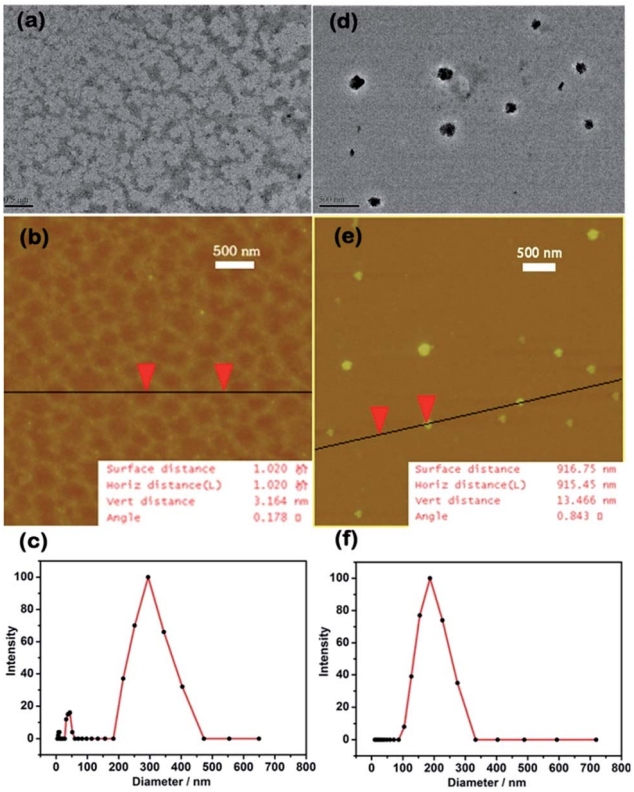

Fig. 1 Typical TEM (a and d), AFM (b and e) images, and DLS results (c and f) of free HAADA (a–c) and DTCD·HAADA nanoparticles (d–f).

Moreover, considering the dynamic equilibrium and non-covalent complexation of β-CD with adamantane, the inclusion efficiency and nanoparticle size were measured by DLS experiments at different concentrations. As can be seen in Table S1 (ESI†), there is a concentration-dependent binding process; that is, the hydrodynamic diameter of the supramolecular assembly DTCD·HAADA increased from 163 to 231 nm as the concentration of DTCD increased from 2.5×10^{-6} to 2.5×10^{-4} M, accompanied by the inclusion efficiency varying from 15% to 80%. As a result, the 1 : 1 ratio of DTCD and HAADA at concentration of 2.5×10^{-4} and 5×10^{-4} M were selected as the optimal condition in the preparation of binary nanoparticles and this was used in the following drug loading and enzyme-responsive releasing studies.

Drug loading behaviors of DTCD·HAADA assembly

After successfully constructing the DTCD·HAADA nanoparticles, we chose the hydrophobic anticancer drug paclitaxel (PTX) as a model to investigate the drug loading and release abilities of the obtained molecular assembly.[19] As shown in

Fig. 2a, a new absorption band centered at 227 nm in the UV/Vis spectrum could be assigned to the entrapped PTX in the DTCD·HAADA assembly, corroborating the successful introduction of hydrophobic drug into aqueous phase. Moreover, by measuring the characteristic absorption at 227 nm in acetonitrile, the photometric standard curve of PTX was obtained (Fig. S6 in ESI†), and the PTX encapsulation and loading efficiency were calculated as 32.0% and 3.0%, respectively (Fig. 2a). Accordingly, the content of PTX in the DTCD·HAADA nanoparticles could be calculated as 64 μg mL^{-1}, which was much larger than the water solubility of free PTX (0.7 μg mL^{-1}).[20] In the control experiments, no drug loading behavior was observed in the presence of HAADA alone, indicating that the polymeric structure is not sufficient to form supramolecular nanoarchitectures and the bridged CD dimer is indispensable to entrap drug molecules in the three-dimensional network of DTCD·HAADA nanoparticles (Fig. 2b).

Drug release behaviors of DTCD·HAADA assembly

After confirming the PTX-loading ability of the obtained nanocarrier, we further investigated the drug release behavior of PTX@DTCD·HAADA assembly in the pH 7.2 phosphate buffer solution (PBS, $I = 0.01$ M) at 37 °C, which is similar to physiological environments. As can be seen from Fig. S7,† free PTX was quickly released and reached equilibrium in about 2 h, but the release rate of PTX@DTCD·HAADA assembly was quite slow under the same experimental condition, suggesting that PTX was tightly bound by the nanocarrier and thus could not be efficiently released without external stimulus. Moreover, the disulfide bond in DTCD provided an excellent cleavage handle for intracellular drug delivery and could be redox-sensitive to some specific reducing agents, such as glutathione and dithiothreitol (DTT).[12] In our case, the cleavage of DTCD's disulfide bonds by DTT was preliminarily examined using electrospray ionization-mass spectrometry (ESI-MS). As expected, a new m/z peak appeared at 1313.4284 after addition of DTT, which could be assigned to the corresponding reduction product MBCD (Fig. S8 in ESI†). Moreover, the morphological change of DTCD·HAADA assembly upon addition of DTT was also characterized by DLS and AFM experiments. When 40 equiv. of DTT (relative to DTCD) was added to DTCD·HAADA solution, a hydrodynamic diameter centered at 123 nm was contributed to the formation of disassembled nanoparticles, and this size was very close to the mixture of HAADA with the reference compound MBCD (Fig. S9a and 9b†). In addition, when DTT was added to the solution of PTX-loaded DTCD·HAADA nanoparticle, no obvious UV/Vis absorption peak was observed at 227 nm, indicating that most PTX was efficiently released from the DTCD·HAADA nanocarriers after the cleavage of disulfide bonds by DTT (Fig. 3a).

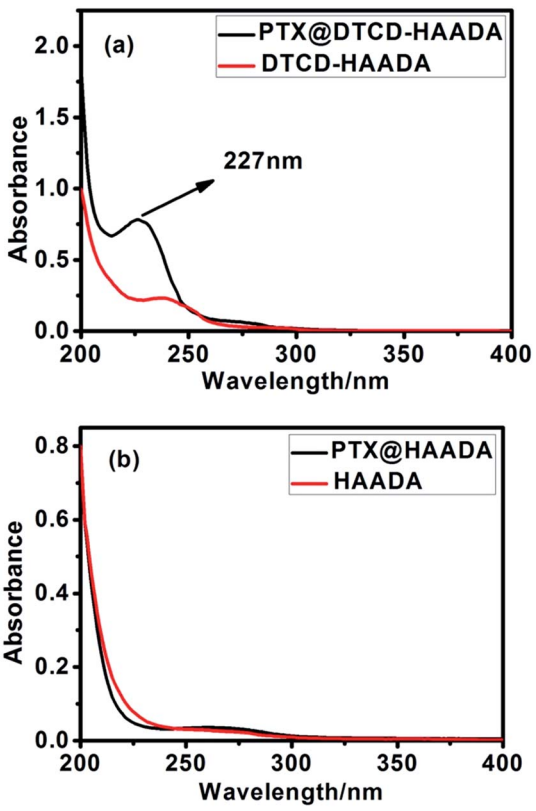

Fig. 2 (a) UV/Vis spectra of free and PTX-loaded DTCD·HAADA nanoparticle after extraction from acetonitrile at 25 °C; (b) UV/Vis spectra of free and PTX-loaded HAADA nanoparticle after extraction from acetonitrile at 25 °C.

Furthermore, we investigated whether DTCD·HAADA nanoparticles could be degraded by the addition of hyaluronidase (HAE). As can be seen in Fig. 4, the morphology of nanoparticles was randomly dispersed after treating with HAE, and a small size distribution was also observed at around 50 nm in the DLS experiments. These morphological information jointly proved that the obtained nanoparticles could be specifically degraded as soon as the polysaccharide backbone of HA was hydrolysed to low-molecular-weight oligomers with assistance of HAE. Furthermore, when HAE was added to PTX-loaded DTCD·HAADA nanoparticles, no UV/Vis absorption band was found at 227 nm, implying that the drug PTX was completely released after the enzyme-triggered degradation of HA skeleton. Moreover, the release efficiency with DTT or HAE was much higher than the one without DTT or HAE, corroborating that the release of hydrophobic drug could be accelerated from the nanocarrier through the disulfide bond cleavage and enzymatic degradation (Fig. S7 in ESI†). Combining these aforementioned results, we can reasonably conclude that the release of anticancer drug in the binary DTCD·HAADA nanoparticles could be modulated by a dual-stimulus responsive manner, that is, the introduction of reductant DTT and HAE to break the disulfide linkage in the bridged bis(β-CD)s and the polysaccharide backbones of HA, respectively.

Anticancer activities *in vitro*

We finally performed cytotoxicity experiments to evaluate the targeting ability and anticancer activities of PTX-loaded DTCD·HAADA nanoparticles *in vitro*, where HA receptor-positive HepG2 (a type of human liver cancer cell line that over-expresses HA receptors on its surface) and HA receptor-

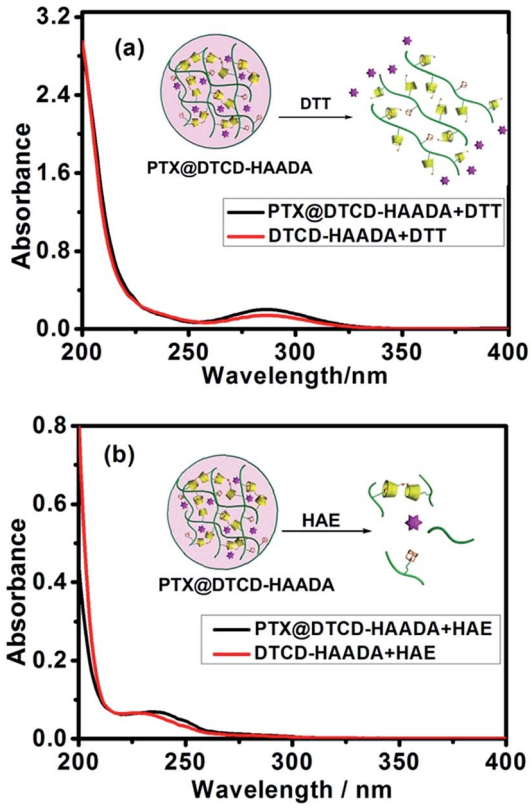

Fig. 3 (a) UV/Vis spectra of PTX-loaded DTCD·HAADA nanoparticle treated by DTT after extraction from acetonitrile at 25 °C; (b) UV/Vis spectra of free and PTX-loaded DTCD·HAADA nanoparticles treated by HAE after extraction from acetonitrile at 25 °C.

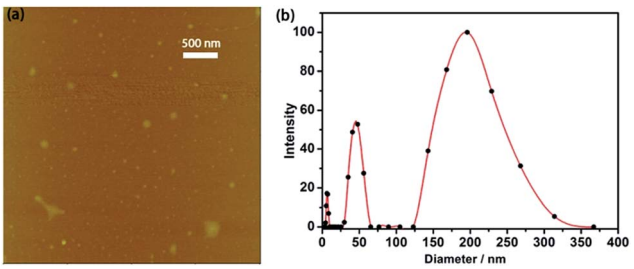

Fig. 4 (a) AFM image and (b) DLS result of DTCD·HAADA nanoparticle treated by HAE.

negative NIH3T3 (mouse embryo NIH3T3 fibroblast cells) were selected as the model cell lines.[21] In our case, the IC_{50} value of PTX-loaded DTCD·HAADA assembly was calculated as 3.4 μg mL^{-1} and the 95% confidence intervals were obtained as 1.7–5.1 μg mL^{-1}. This obtained IC_{50} value was similar to free PTX toward HepG2 cells (IC_{50} = 3.2 μg mL^{-1})[21] after incubation for 24 h (Fig. S10 in ESI†). Moreover, as shown in Fig. 5, free PTX displayed a similar cytotoxicity toward both normal and cancer cells (*ca.* 67.3%, 65.1%), whereas the binary DTCD·HAADA nanocarrier was basically nontoxic and the cellular viability maintained above 70%. In contrast, when PTX was encapsulated by the DTCD·HAADA nanoparticles, the drug-loaded nanoassembly showed a better anticancer activity toward

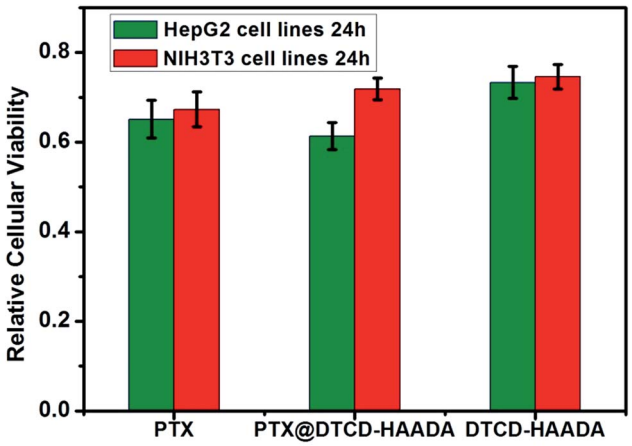

Fig. 5 Relative cellular viability of HepG2 and NIH3T3 cell lines after treatment with free PTX, DTCD·HAADA nanocarrier, and PTX-loaded nanoparticles in 24 h incubation ([PTX] = 2.5 μg mL^{-1}, and [DTCD·HAADA] = 80 μg mL^{-1}).

HepG2 cancer cell line with 61.3% cellular viability after 24 h, which was relatively lower than the one toward NIH3T3 normal cell line (71.9%). These results were mainly contributed to the highly selective binding between HA units on the DTCD·HAADA nanoparticles and HA receptors on the HepG2 cancer cell surface and the facile release of PTX by the endogenous glutathione and HAE in the cell cytosol,[22,23] thus facilitating the subsequent incorporation of PTX@HA-CD-NPs into the cancer cells by HA-mediated endocytosis process.

Conclusions

In summary, we developed a dual-stimulus responsive drug delivery system by the noncovalent association of adamantane-grafted hyaluronic acid (HAADA) with disulfide-containing bridged bis(β-CD)s (DTCD). The hydrophobic anticancer drug PTX can be encapsulated in the 3D network of DTCD·HAADA nanoparticles with a moderate loading efficiency. Owing to the redox-active disulfide bonds in DTCD and the biocompatible polysaccharide skeleton in HA, the release of PTX could be readily achieved by the disulfide bond cleavage with DTT and the enzymatic degradation with HAE. Gratifyingly, the resultant drug-loaded nanoassembly with cell-specific targeting ability exhibited relatively better anticancer activity toward HepG2 cancer cells than free PTX *in vitro*. These results may promote the bridged bis(β-CD)s-based polysaccharide nanoparticle as a safe and promising nanocarrier, thus providing a new way to create more intelligent biomaterials in oncological treatment. Further studies on the complexation of HA derivatives with other functional bridged bis(β-CD)s are currently in progress.

Acknowledgements

We thank the National Natural Science Foundation of China (No. 21432004, 21472100, and 91527301) for financial support.

Notes and references

1 (*a*) J. Nicolas, S. Mura, D. Brambilla, N. Mackiewicz and P. Couvreur, *Chem. Soc. Rev.*, 2013, **42**, 1147–1235; (*b*) N. Saleh, A. L. Koner and W. M. Nau, *Angew. Chem., Int. Ed.*, 2008, **47**, 5398–5401.

2 (*a*) X.-L. Qiu, Q.-L. Li, Y. Zhou, X.-Y. Jin, A.-D. Qi and Y.-W. Yang, *Chem. Commun.*, 2015, **51**, 4237–4240; (*b*) L. Su, W. Zhang, X. Wu, Y. Zhang, X. Chen, G. Liu, G. Chen and M. Jiang, *Small*, 2015, **11**, 4191–4200; (*c*) S. Aryal, J. J. Grailer, S. Pilla, D. A. Steeber and S. Gong, *J. Mater. Chem.*, 2009, **19**, 7879–7884.

3 M.-Y. Lee, S.-J. Park, K. Park, K. S. Kim, H. Lee and S. K. Hahn, *ACS Nano*, 2011, **5**, 6138–6147.

4 (*a*) X. Ma and Y. Zhao, *Chem. Rev.*, 2015, **115**, 7794–7839; (*b*) Y.-W. Yang, Y.-L. Sun and N. Song, *Acc. Chem. Res.*, 2014, **47**, 1950–1960.

5 Q. Duan, Y. Cao, Y. Li, X. Hu, T. Xiao, C. Lin, Y. Pan and L. Wang, *J. Am. Chem. Soc.*, 2013, **135**, 10542–10549.

6 (*a*) K. M. Park, J.-A. Yang, H. Jung, J. Yeom, J. S. Park, K.-H. Park, A. S. Hoffman, S. K. Hahn and K. Kim, *ACS Nano*, 2012, **6**, 2960–2968; (*b*) Y. Luo, M. R. Ziebell and G. D. Prestwich, *Bioconjugate Chem.*, 1999, **10**, 755–763.

7 (*a*) S.-Y. Han, H. S. Han, S. C. Lee, Y. M. Kang, I.-S. Kim and J. H. Park, *J. Mater. Chem.*, 2011, **21**, 7996–8001; (*b*) H. Lee, K. Lee and T. G. Park, *Bioconjugate Chem.*, 2008, **19**, 1319–1325.

8 S. Sreejith, X. Ma and Y. Zhao, *J. Am. Chem. Soc.*, 2012, **134**, 17346–17349.

9 Y. Chen and Y. Liu, *Adv. Mater.*, 2015, **27**, 5403–5409.

10 Y. Chen and Y. Liu, *Acc. Chem. Res.*, 2006, **39**, 681–691.

11 N. Li, Y. Chen, Y.-M. Zhang, Y. Yang, Y. Su, J.-T. Chen and Y. Liu, *Sci. Rep.*, 2014, **4**, 4164.

12 (*a*) D. P. Jones, J. L. Carlson, P. S. Samiec, P. Sternberg, V. C. Mody, R. L. Reed and L. A. S. Brown, *Clin. Chim. Acta*, 1998, **275**, 175–184; (*b*) A. N. Koo, H. J. Lee, S. E. Kim, J. H. Chang, C. Park, C. Kim, J. H. Park and S. C. Lee, *Chem. Commun.*, 2008, 6570–6572.

13 M. W. Ambrogio, T. A. Pecorelli, K. Patel, N. M. Khashab, A. Trabolsi, H. A. Khatib, Y. Y. Botros, J. I. Zink and J. F. Stoddart, *Org. Lett.*, 2010, **12**, 3304–3307.

14 I. Rivkin, K. Cohen, J. Koffler, D. Melikhov, D. Peer and R. Margalit, *Biomaterials*, 2010, **31**, 7106–7114.

15 (*a*) D. Peer and R. Margalit, *Int. J. Cancer*, 2004, **108**, 780–789; (*b*) G. Bachar, K. Cohen, R. Hod, R. Feinmesser, A. Mizrachi, T. Shpitzer, O. Katz and D. Peer, *Biomaterials*, 2011, **32**, 4840–4848.

16 Y. Yang, Y.-M. Zhang, Y. Chen, J.-T. Chen and Y. Liu, *J. Med. Chem.*, 2013, **56**, 9725–9736.

17 Y. Li, D. Maciel, J. Rodrigues, X. Shi and H. Tomás, *Chem. Rev.*, 2015, **115**, 8564–8608.

18 (*a*) Y. Liu, Y.-W. Yang and Y. Chen, *Chem. Commun.*, 2005, **41**, 4208–4210; (*b*) Y.-M. Zhang, Y. Cao, Y. Yang, J.-T. Chen and Y. Liu, *Chem. Commun.*, 2014, **50**, 13066–13069.

19 (*a*) A. M. C. Yvon, P. Wadsworth and M. A. Jordan, *Mol. Biol. Cell*, 1999, **10**, 947; (*b*) R. V. Chari, *Adv. Drug Delivery Rev.*, 1998, **31**, 89.

20 A. E. Mathew, M. R. Mejillano, J. P. Nath, R. H. Himes and V. J. Stella, *J. Med. Chem.*, 1992, **35**, 145–151.

21 (*a*) H. He, S. Chen, J. Zhou, Y. Dou, L. Song, L. Che, X. Zhou, X. Chen, Y. Jia, J. Zhang, S. Li and X. Li, *Biomaterials*, 2013, **34**, 5344–5358; (*b*) Y. Luo, N. J. Bernshaw, Z.-R. Lu, J. Kopecek and G. D. Prestwich, *Pharm. Res.*, 2002, **19**, 396–402; (*c*) H. Wang, K. Liu, K.-J. Chen, Y. Lu, S. Wang, W.-Y. Lin, F. Guo, K. Kamei, Y.-C. Chen, M. Ohashi, M. Wang, M. A. Garcia, X.-Z. Zhao, C. K.-F. Shen and H.-R. Tseng, *ACS Nano*, 2010, **4**, 6235–6243.

22 (*a*) V. B. Lokeshwar, B. L. Lokeshwar, H. T. Pham and N. L. Block, *Cancer Res.*, 1996, **56**, 651–657; (*b*) R. Stern, *Semin. Cancer Biol.*, 2008, **18**, 275–280.

23 (*a*) A. Meister and M. E. Anderson, *Annu. Rev. Biochem.*, 1983, **52**, 711–760; (*b*) R. Hong, G. Han, J. M. Fernández, B.-J. Kim, N. S. Forbes and V. M. Rotello, *J. Am. Chem. Soc.*, 2006, **128**, 1078–1079; (*c*) S. Takae, K. Miyata, M. Oba, T. Ishii, N. Nishiyama, K. Itaka, Y. Yamasaki, H. Koyama and K. Kataoka, *J. Am. Chem. Soc.*, 2008, **130**, 6001–6009.

